Contents lists available at ScienceDirect

Inorganica Chimica Acta

journal homepage: www.elsevier.com/locate/ica

Review article

From traditional PTA to novel CAP: A comparison between two adamantane cage-type aminophosphines

Antonella Guerriero *, Luca Gonsalvi *

Consiglio Nazionale delle Ricerche (CNR), Istituto di Chimica dei Composti OrganoMetallici (ICCOM), Via Madonna del Piano 10, 50019 Sesto Fiorentino (Florence), Italy

ARTICLE INFO

Dedicated to our colleague and friend Dr. Maurizio Peruzzini in occasion of his 65th birthday and to celebrate his outstanding scientific career.

Keywords:
Water-soluble ligands
Cage aminophosphines
Coordination chemistry
Homogeneous catalysis
Reactivity
Medicinal chemistry

ABSTRACT

The cage-like water-soluble monodentate phosphine 1,3,5-triaza-7-phosphatricyclo[3.3.1.1]decane (also known as 1,3,5-triaza-7-phosphadamantane, PTA) has been known for many years and has been widely used in organometallic chemistry due to its ability to solubilize and stabilize transition metal complexes in aqueous phase. Through synthetic modifications, many PTA derivatives have also been obtained and used as coordinating ligands. The numerous PTA metal compounds produced have found application in particular in catalysis, but also in medicinal chemistry and for photoluminescent purposes. More recently, the synthesis of 1,4,7-triaza-9-phosphatricyclo[5.3.2.1]tridecane, abbreviated as CAP, has been reported. This phosphine, that can be considered as a higher homologue of PTA, has already shown interesting properties, sometimes considerably different from PTA. This minireview summarizes and compares the properties and reactivity of the two ligands and the activity in catalysis and in medicinal chemistry of the transition metal complexes described so far in the literature.

1. Introduction

The use of organophosphines as ancillary ligands is an established approach in organometallic chemistry, due to their ability to stabilize low metal oxidation states and to their synthetic versatility, in turn allowing for fine tuning of the electronic and steric properties as well as the solubility of the corresponding metal complexes. On the other hand, the need for more sustainable chemical processes has driven both academia and industry to study the development of systems active in aqueous solution, as water is a safer and green alternative to toxic organic solvents [1,2]. One of the strategies to convey organometallic compounds in aqueous phase is to use hydrophilic ligands [3] and among them the neutral adamantane-like phosphine 1,3,5-triaza-7-phosphadamantane, also known as PTA (**1**, Fig. 1), has been of great interest for many research groups worldwide, owing to its attractive combination of a low sterically demanding structure and a high chemical and thermal stability, further that its high solubility in water. The coordination chemistry of PTA and its derivatives to the majority of transition metals has been largely investigated and, beside to the main use in catalysis, the application of the resulting complexes in luminescence studies, in medicinal chemistry and in 1D and 3D materials have been reported in the literature over the years [4]. Through the structural modifications of PTA, involving *N*-quaternization (lower rim functionalization) and introduction of a side arm in C-6 position (upper rim functionalization), many derivatives have been synthesized with different electronic, steric, solubility and binding properties [5].

Our research group worked for many years on PTA chemistry, in particular on its synthetic modifications and on the synthesis of transition metal complexes active in homogeneous catalysis and medicinal chemistry. More recently, we turned our interest to the chemistry of new cage-like adamantane phosphines. A higher homologue of PTA, namely 1,4,7-triaza-9-phosphatricyclo[5.3.2.1]tridecane, abbreviated as CAP (**2**, Fig. 1), built on a triazacyclononane macrocycle embedded into the cage, has been described for the first time in 2015 by Britvin and coworkers [6] Although structurally very similar, the two ligands show remarkable differences in their conformational behavior, reactivity and coordination chemistry. In the last few years, some transition metal compounds bearing CAP have also been described and investigated for their potential catalytic and medicinal applications. The aim of this review article is to highlight the main similarities and differences between the two phosphines and their reactivities, often reflected in unusual ^{31}P NMR chemical shift values (Table 1), as well as to compare the

* Corresponding authors.
E-mail addresses: antonella.guerriero@iccom.cnr.it (A. Guerriero), l.gonsalvi@iccom.cnr.it (L. Gonsalvi).

https://doi.org/10.1016/j.ica.2021.120251
Received 25 November 2020; Received in revised form 29 December 2020; Accepted 31 December 2020

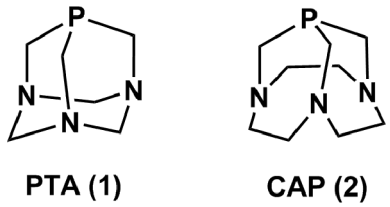

Fig. 1. Drawings of PTA (**1**) and CAP (**2**) aminophosphine ligands.

many organic solvents including DMSO, acetone, chloroform and dichloromethane.

The cone angle of PTA is rather small, with a measured value of 103°, lower than that of other alkyl phosphines such as PEt_3 (132°), PMe_3 (118°) or PCy_3 (170°), denoting a low steric hindrance character of this ligand. Regarding the characterization in solution of **1**, its $^{31}P\{^1H\}$ NMR spectrum in D_2O shows a singlet at −98.3 ppm slightly shifted to −101.0 ppm in $CDCl_3$, whereas in the ^1H NMR spectrum a broad singlet at 4.43 ppm due to N-CH_2-N and a doublet at 3.90 ppm ($^2J_{HP}$ = 9.0 Hz)

Table 1
$^{31}P\{^1H\}$ NMR chemical shift values of PTA, CAP, derivatives and selected complexes.

Compound	$^{31}P\{^1H\}$NMR chemical shifts (δ, ppm)	Solvent	Reference
PTA (**1**)	−98.3, s	D_2O	[8]
	−101.0, s	$CDCl_3$	
CAP (**2**)	46.7, s	D_2O	[6,10]
	52.8, s	$CDCl_3$	
(PTA-H)Cl (**3**)	−89.9, s	D_2O	[14b]
PTA(O) (**4**)	−2.5, s	D_2O	[7,8]
[PTA(*N*-Me)]I (**6**)	−86.1, s	DMSO-d_6	[8]
[PTA(*N*,*N*′-Me)$_2$](OTf)$_2$ (**7**)	−80.8, s	D_2O	[20]
[PTA(O)(*N*-Me)]I (**8**)	−1.3, s	D_2O	[17b]
(CAP-H)Cl (**9**)	25.2, s	D_2O	[6]
(CAP-H$_2$)Cl$_2$ (**10**)	12.8, s	D_2O	[6]
(CAP-H$_3$)]Cl$_3$ (**11**)	12.3, s	D_2O	[6]
CAP(O) (**12**)	52.0, s	D_2O	[11]
[(CAP-H$_2$)(O)]Cl$_2$ (**13**)	32.1, s	D_2O	[11]
[CAP(O)(*N*-OH)$_2$]$^{2+}$ (**14**)	15.9, s	D_2O	[11]
[CAP(*P*-Me)]I (**15**)	25.6, s	D_2O	[11]
[CAP(*P*,*N*-Me$_2$)]I$_2$ (**16**)	18.9, s	D_2O	[11]
[(CAP-H$_2$)(*P*-Me)](Cl)$_2$I (**17**)	24.7, s	D_2O	[11]
[CAP(O)(*N*-Me$_2$)]I$_2$ (**18**)	19.8, s	D_2O	[11]
[RuCl$_2$(η^6-*p*-cymene)(PTA)] (**19**)	−36.6, s	$CDCl_3$	[31]
[RuCl(η^6-*p*-cymene)(PTA)$_2$]BF$_4$ (**20**)	−33.0, s	D_2O	[30]
[RuCl$_2$(η^6-*p*-cymene)(CAP)] (**21**)	52.8, s	$CDCl_3$	[10]
[RuCl(η^6-*p*-cymene)(MeCN)(CAP)]PF$_6$ (**22**)	48.2 s, −144.3 sept ($^1J_{PF}$ = 707.8 Hz)	Acetone-d_6	[10]
[RuCl(η^6-*p*-cymene)(CAP)$_2$]PF$_6$ (**23**)	51.6 s, −144.3 sept ($^1J_{PF}$ = 707.5 Hz)	Acetone-d_6	[10]
[RuH(η^6-*p*-cymene)(CAP)$_2$]PF$_6$ (**24**)	67.5 s, −149.5 sept ($^1J_{PF}$ = 711.1 Hz)	CD_2Cl_2	[33]
[RuCl$_2$(η^6-*p*-cymene)(PTA-H)](BPh$_4$) (**25**)	22.1 s	Acetone-d_6	[35]
[RuCl$_2$(η^6-*p*-cymene)(CAP-H)](BPh$_4$) (**26**)	61.1 s	CD_3CN	[34]
	58.4 s	DMSO-d_6	
cis-[PdCl$_2$(CAP)$_2$]·2H$_2$O (**27**)	43.0 s	D_2O	[56]
cis-[PdCl$_2$(CAP-H)(CAP-H$_2$)]Cl$_3$·3H$_2$O (**28**)	42.8 s	D_2O	[56]
cis-[PdCl$_2$(CAP-H$_2$)$_2$]Cl$_4$·4.5H$_2$O (**29**)	42.6 s	D_2O	[56]
cis-[PtCl$_2$(CAP-H$_2$)$_2$]Cl$_4$·4.5H$_2$O (**30**)	22.6, sat. 32.1, 13.0 ppm ($^1J_{Pt\text{-}P}$ = 3093 Hz)	D_2O	[56]
[^{99}Tc(PTA)(CO)$_5$]OTf (**31a·OTf**)	−58.5 s	CD_3CN	[58]
[^{99}Tc(CAP)(CO)$_5$]OTf (**32a·OTf**)	−48.8 s	CD_3CN	[58]

properties of their corresponding transition metal complexes reported in the literature so far and their activity when applied in the same catalytic processes or for the same medical purposes.

2. Synthesis, characterization and structural properties of PTA and CAP

The synthesis of PTA (**1**) was described for the first time by Daigle in 1974, by condensation reaction of trishydroxymethylphosphine (THP, [P(CH_2OH)$_3$]), with hexamethylenetetramine or, alternatively, with an ammonia solution, in the presence of formaldehyde [7]. The early yield of *ca.* 40% was later increased up to 80% by first obtaining *in situ* the phosphine THP in the reaction of the air-stable and commercially available tetrakis(hydroxymethyl)phosphonium chloride (THPC) with sodium hydroxide (Scheme 1) [8]. After crystallization in hot ethanol or acetone, PTA was isolated as a pure crystalline white solid, which, contrary to other alkyl phosphines such as PMe_3 and PEt_3, resulted to be highly stable to air and moisture, and also thermally stable decomposing at temperatures higher than 260 °C. In addition to its high solubility in water at room temperature with $S(H_2O)_{25°C}$ = 1.5 M, ca. 235 g/L, PTA is also well soluble in MeOH and EtOH and less soluble in heavier alcohols such as 2-propanol, *n*-butanol and THF. It also shows good solubility in due to P-CH_2-N are observed [8].

The new ligand CAP (**2**) features a tris(homoadamantane) cage which can be considered a structural intermediate between those of PTA and of the unstable Verkade's aminophosphine [9]. Indeed, CAP is similar to the latter for the presence of the triazacyclononane ring in its cage and to PTA for the same environment at the phosphorus atom which is connected with the nitrogen atoms through three bridging methylene groups. CAP was firstly prepared by a Mannich-type condensation of 1,4,7-triazacyclononane (TACN) and THP in MeOH at room temperature. After slow evaporation of the reaction solution in air, **2** was obtained as dodecahedral white crystals (Fig. 2) in *ca.* 45% yield. The low yield was justified by the authors with the formation of a large amount of amorphous byproducts, likely polymeric in nature [6]. Based on our experience on PTA preparation, this synthetic procedure was slightly modified by us some time later. Thus, THPC (80% solution in water) was first treated with NaOH (1.6 M) to obtain THP *in situ*, which was directly reacted with TACN at room temperature in aqueous solution. This solution was then extracted with $CHCl_3$ and after crystallization of the crude product from hot ethanol, CAP was obtained as a white crystalline pure solid (Scheme 1) [10]. Although this procedure does not increase the final yield as the formation of the unidentified amorphous solid could not be avoided, it has the advantage of using the easier-to-

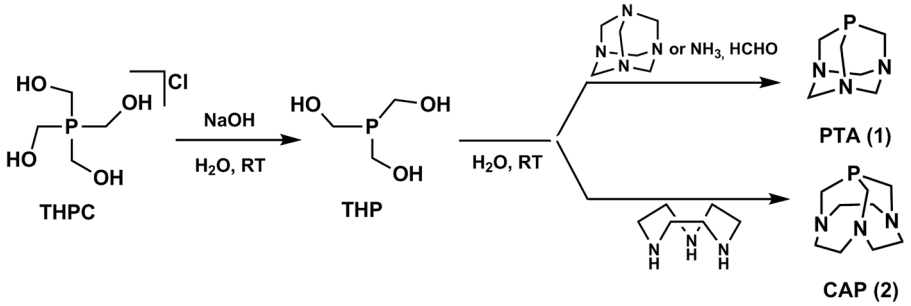

Scheme 1. Synthesis of **1** and **2**.

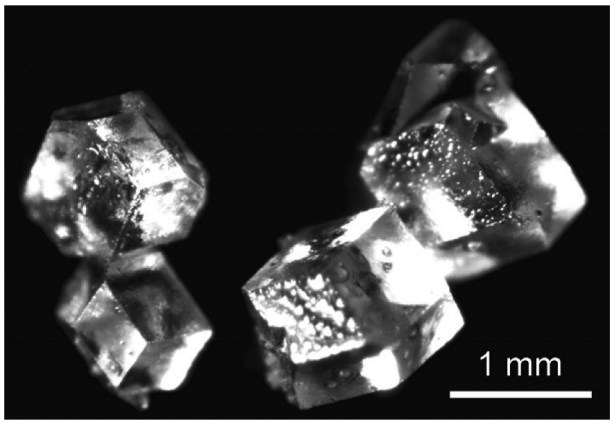

Fig. 2. Dodecahedral crystals of **2**. Reprinted with permission from [6]. Copyright 2015 American Chemical Society.

handle THPC instead of the air sensitive THP, of using water as solvent instead of an organic solvent and a easier and faster workup.

CAP is stable in air both as solid and in solution and has a thermal stability comparable with that of PTA. Furthermore, it has a melting point of *ca.* 50 °C and evaporates under Argon atmosphere at a temperature between 200 and 300 °C without decomposition. **2** is soluble in water with $S(H_2O)_{25°C} = 0.1$ M, ca. 2 g/100 mL, that is ca. an order of magnitude lower than the value reported for **1**. CAP is also soluble in alcohols such as MeOH, EtOH and ^{i}PrOH and in chlorinated solvents such as $CHCl_3$ and CH_2Cl_2, while it shows no solubility in acetone, THF, benzene, toluene and hexane [6]. The cone angle of CAP is calculated at 109° confirming, as for PTA, the low steric demand nature of this ligand, whereas the DFT calculations of TEP (Tolman's electronic parameter), a parameter used to conventionally estimate the electron-donating ability of phosphines, gave a value of 2056.8 cm^{-1}. The lower value of TEP for CAP compared to that calculated for PTA (2070.2 cm^{-1}) implies that ligand **2** has an electron-donating ability at the P atom higher than that of **1** and closer to that of stronger electron donor phosphines such as P(*t*-Bu)$_3$ and PCy_3. Thus, based on the electron donicity properties, CAP can be considered as the water-soluble counterpart of P(*t*-Bu)$_3$ and PTA as the water-soluble counterpart of PPh_3 (Fig. 3).

Although similar from the sterical point of view, the significantly different electronic properties of PTA and CAP are also responsible of the large differences in the ^{31}P NMR chemical shifts (Table 1). In fact, the $^{31}P\{^1H\}$ NMR spectrum of CAP in D_2O shows a singlet at 46.7 ppm, a value exceedingly different from that of PTA (−98.3 ppm) and more similar to that of P(*t*-Bu)$_3$ (62.2 ppm in toluene-d_8). This large magnitude of ^{31}P upfield shifting for CAP and its derivatives relative to PTA ($\Delta\delta = -145.0$ ppm) has been explained by Britvin and co-workers as a consequence of the formation of intramolecular lone pair interactions in CAP, a phenomenon previously reported in azaphosphatrane systems to explain their NMR anomalies [11]. Indeed, both in CAP and in azaphosphatranes some substitutions give a pyramidal *out-in* inversion at one of the N atoms resulting in the formation of short intramolecular P···N and N···N linkages. Through DFT calculation studies based on the electron density distribution analysis, the authors revealed that the P and N centers of the tris(homoadamantane) cage of **2** exhibit equal electron donicity and the enhancement of P-donicity of CAP compared with that of PTA is likely correlated to the occurrence of weak but

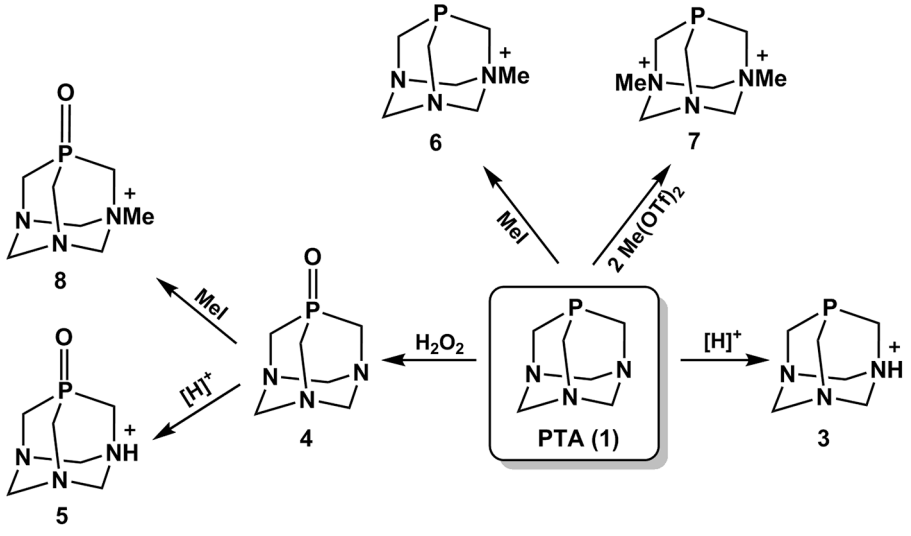

Scheme 2. Protonation, oxidation and methylation reactions of **1**.

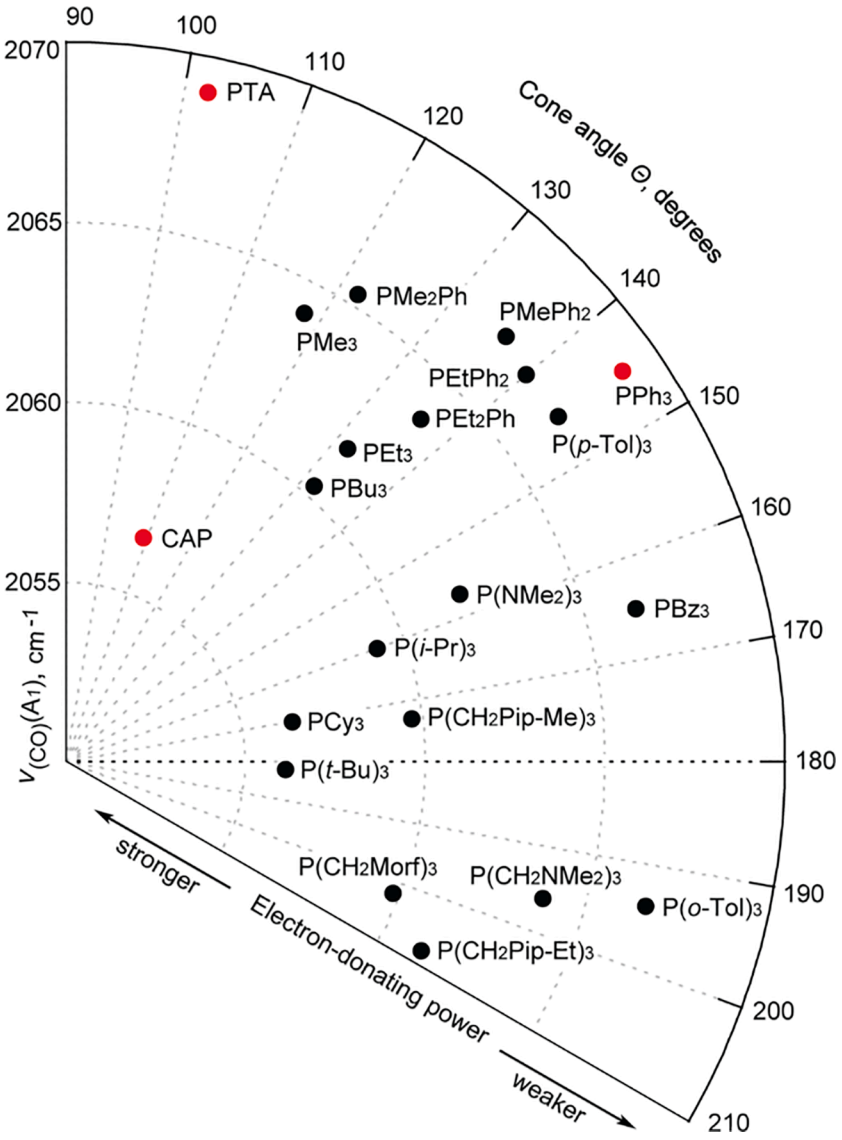

Fig. 3. Polar stereoelectronic map of phosphine ligands, showing the correlation of electron-donating power to Tolman's electronic parameter $\nu(CO)(A_1)$ and cone angle Θ (°). Reprinted with permission from [6]. Copyright 2015 American Chemical Society.

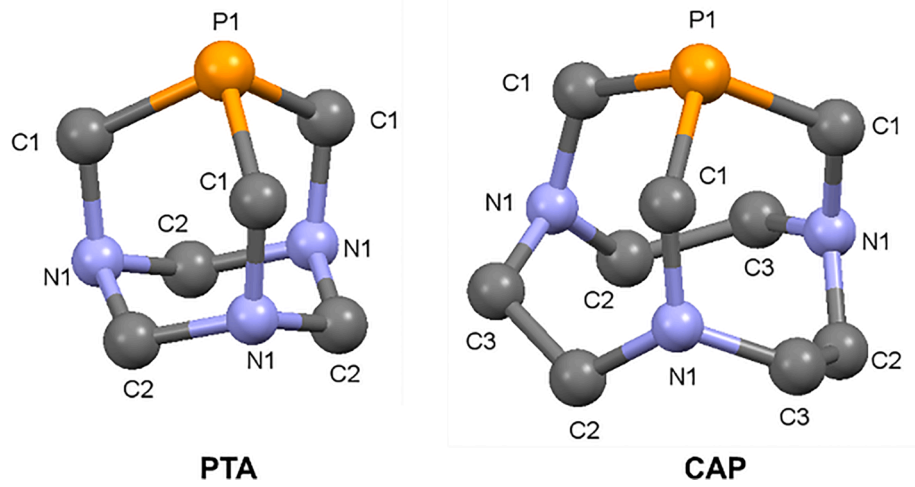

Fig. 4. X-ray crystal structures of PTA and CAP. Drawings by CCDC Mercury® 3.9.

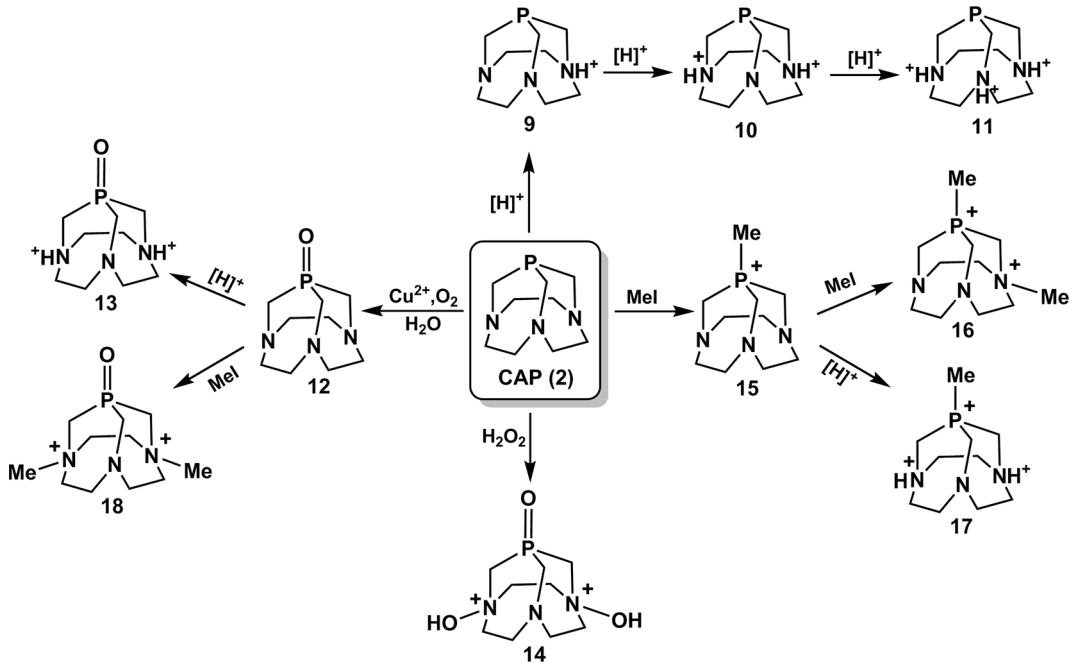

Scheme 3. Protonation, oxidation and methylation reactions of **2**.

definite P···N intercage interactions, resulting in accumulation of electron density at the centre of the cage.

Both PTA and CAP were characterized in the solid state by X-ray crystal structural determination (Fig. 4). In both cases a [333] conformation is present. The characteristic bondlengths in PTA are P1—C1 = 1.8661(7) Å, N1—C1 = 1.4721(10) Å and N1—C2 = 1.4672(5) Å. For CAP, the main bondlengths are P1—C1 = 1.8697(8) Å, N1—C1 = 1.4472 (10) Å, N1—C2 = 1.4544(9) Å and N1—C3 = 1.4517(8) Å. As expected, the higher cage flexibility of CAP is reflected in the bond distances of the lower triazacyclononane rim.

In conclusion, the ^{31}P NMR chemical shifts of CAP and its derivatives (*vide infra*) are greatly affected by their conformational and stereoelectronic properties, which are in turn governed by the cage conformation. In the solid state, the 9-membered ring in CAP maintains the same [333] conformation [12] of that of free TACN [13]. This conformation is the most energetically favored among the nine-membered macrocycles giving to these rings a high degree of conformational freedom. For this reason, one of the main difference between the two phosphines is that CAP is characterized by a "semi-flexible" cage, while PTA is known for the rigidity of its adamantane skeleton.

3. A comparison of selected reactivities between PTA and CAP

Despite having similar solubility, stability and structural properties, the stereoelectronic differences between PTA and CAP lead to evident differences in reactivity such as in protonation, oxidation or alkylation reactions [11].

In aqueous solutions with a pH lower than 6.5, PTA is regioselectively protonated at one nitrogen atom giving the corresponding ammonium derivative $(PTA\text{-}H)^+$ (**3**) (Scheme 2) [4a]. As demonstrated experimentally and by DFT calculations, a further *N*-protonation is thermodynamically less favored because changes in hybridization of nitrogen centers cause severe distortions of the adamantane cage resulting in a decrease of the overall stability. On the other hand, whereas PTA is known as a monoacidic base with a acidity constant pK_{a1} measured by different authors at 5.7 [14a] and 6.0 [14b], its homologue CAP behaves as a triacidic amine base, being able to be protonated to all three nitrogen atoms [6]. The calculated pK_{a1} and pK_{a2} of CAP resulted 6.2 and 2.9 respectively, and through acid-base titrations the sequential formation of the cations $(CAP\text{-}H)^+$ (**9**) and $(CAP\text{-}H_2)^{2+}$ (**10**) (Scheme 3) has been observed. The remaining third nitrogen site is only weakly basic but the triprotonated ion $(CAP\text{-}H_3)^{3+}$ (**11**) has also been isolated from highly acidic solutions and confirmed by X-ray diffraction analysis. The polyamine behavior showed by CAP can be related to its high degree of conformational flexibility due to the nine-membered TACN ring allowing the existence of a variety of distorted conformers [12,15]. Reaction of PTA with strong acids (excess) generally leads to cage opening [4].

Furthermore, when an aqueous solution of **11** was added to a solution of $HAuCl_4$, the immediate formation of gold nanoparticles with dimensions between 5 and 10 nm was observed [6]. This ability to reduce Au(III) to Au(0) is unusual for tertiary phosphines, which commonly afford phosphine-Au(I) complexes if reacted with Au(III) precursors [16]. Aside from **11**, CAP can promote the oxidative dissolution of nanocrystalline Au(0) to give CAP-Au(I) complexes and the ability to displace cyanide from $[Au(CN)_2]$ forming the cation $[Au(CAP)_3]^+$ [6]. As in the case of free PTA and CAP, their *N*-protonated derivatives show different behavior in the $^{31}P\{^1H\}$ NMR spectra. Whereas (PTA-H)Cl (**3·Cl**) is characterized by a singlet at −89.9 ppm (D_2O), a chemical shift value only slightly different from that of unmodified PTA (−98.3 ppm) [14b], $^{31}P\{^1H\}$ NMR chemical shifts of CAP derivatives are highly influenced by protonation giving peaks in D_2O at 12.8 ppm for $(CAP\text{-}H_2)Cl_2$ (**10·Cl$_2$**) and 12.3 ppm for $(CAP\text{-}H_3)Cl_3$ (**11·Cl$_3$**) corresponding to a $\Delta\delta$ with **2** of −33.9 and −34.4 ppm, respectively [6].

The oxidation of the phosphorus center can be accomplished in both **1** and **2** but under different reaction conditions. PTA can be easily oxidized to the corresponding P-oxide PTA(O) (**4**) (Scheme 2) in the presence of hydrogen peroxide, nitric acid [17a] or nitrogen tetraoxide solutions [17b]. The P═O bond formation leads to a large change in $^{31}P\{^1H\}$ NMR chemical shift compared to PTA with a singlet detected at −2.49 ppm (D_2O) [7,8]. PTA(O), which was sometimes observed to form as by-product in the course of synthetic or catalytic reactions involving PTA, is thermally stable, decomposing at temperatures higher than 260 °C and less soluble in water than **1** [8]. Oxidation of the P centre causes a decrease of basicity of the nitrogen atoms in **4** and, as in the case of **1**, reactions of PTA(O) with H^+ sources lead only to the monoprotonated cation [(PTA-H)(O)] (**5**, Scheme 2). Through PTA(O) reduction,

using polymethylhydrosiloxane (PMHS) as reductant in a metal-free process run under nitrogen at 220 °C temperature, it is possible to recover PTA [18].

The P-oxide derivative of CAP, namely CAP(O) (**12**, Scheme 3), was obtained by slow aerial oxidation of an aqueous solution of **2** in the presence of catalytic amounts of Cu^{2+} salts [11]. Compound **12** retains the same [333] conformation of the free ligand **2**, as confirmed by the slight shift of the signal in the $^{31}P\{^{1}H\}$ NMR spectrum (52.0 ppm) and, like CAP, it can be protonated with HCl at two nitrogen sites, affording the dicationic species $[(CAP\text{-}H_2)(O)]Cl_2$ (**13**, Scheme 3). Treatment of **2** with an aqueous solution of H_2O_2 does not lead to **12** as observed for PTA, but rather to the CAP(O)-dihydroxyammonium dication $[CAP(O)(N\text{-}OH)_2]^{2+}$ (**14**, Scheme 3). The third nitrogen atom of the cage is not oxidized, and this is likely due to the severe distortion suffered by **14**. The formation of this derivative is not an unexpected result by considering that hydrogen peroxide is known to be used in the synthesis of *N*-oxides [19], but it represents another diversity point between CAP and PTA reactivities.

When reacted with MeI in acetone solution under reflux conditions, PTA is regioselectively alkylated at the nitrogen atom affording the derivative [PTA(*N*-Me)]I (**6**, Scheme 2) [17b]. This *N*-alkyl salt results to be stable in air and water, but less soluble in organic solvents than PTA. The reactivity of **6** differs from that of **1** and, for example, P-oxidation with H_2O_2 does not occur, hence the P atom maintains the same coordination ability of PTA to transition metals. If reacted with MeI, also **4** is methylated to one nitrogen site affording compound [PTA(O)(*N*-Me)]I (**8**) [17a]. On the other hand, reaction of **1** with two equiv. of $MeO\text{-}SO_2CF_3$ in acetone gives the *N*-dimethylated derivative $[PTA(N,N'\text{-}Me)_2](OTf)_2$ (**7**, Scheme 2) [20]. By using other alkylating agents, such as EtI [21], $PhCH_2Cl$ [14b,22] or $I(CH_2)_4I$ [23], the corresponding *N*-alkylated-PTA salts are always obtained. *P*-alkylation is not obtained directly from PTA, but only by refluxing an acetone solution of the precursor $[RP(CH_2OH)_3]Cl$ (R = Me, Et, Ph, Bz, Cy) in the presence of ammonium acetate and formaldehyde [24].

Contrary to PTA, by reacting CAP with MeI, the *P*-methylated cation [CAP(P-Me)]I (**15**) is readily obtained (Scheme 3). This remarkably different behavior between the two phosphines is due to their different electronic properties and, in particular, different electron donicity of P and N atoms, as discussed above. As observed for **12**, compound **15** maintains the highly symmetric [333] conformation of the 9-membered macrocyle [11] and in its ^{1}H NMR spectrum in D_2O, the P-CH_3 group is detected as a doublet at 1.43 ppm ($^{2}J_{HP} = 17.3$ Hz) which is in line with the signal of P-CH_3 of the corresponding *P*-methylated PTA derivative (doublet at 1.82 ppm, $^{2}J_{HP} = 15.6$ Hz) [25]. By reaction with diluted HCl solutions, **15** is easily protonated yielding the trication $[(CAP\text{-}H_2)(P\text{-}Me)](Cl)_2I$ (**17**), while if reacted with an equimolar amount of MeI in methanol solution, it affords the *P*,*N*-methylated dication $[CAP(P,N\text{-}Me_2)]I_2$ (**16**, Scheme 3). Further alkylations are not observed in **15** even in the presence of an excess of methyl iodide. This behavior is in contrast with that shown by **12**, which forms the *N*,*N*′-methylated dication $[CAP(O)(N\text{-}Me_2)]I_2$ (**18**) when treated with an excess of MeI [11].

In the solid state, whereas the conformation of the nine-membered ring in the structures of parent CAP and triprotonated ion $(CAP\text{-}H_3)^{3+}$ can be designated as highly symmetrical [333], the protonation of the two nitrogen sites of CAP results in severe distortion of the macrocycle and the whole cage of $(CAP\text{-}H_2)^{2+}$ resulting in a [1233] conformation, with the concave cage topology at the non-protonated nitrogen site (Fig. 5). Main bondlengths for $(CAP\text{-}H_2)^{2+}$ are P1—C1 = 1.844(2) Å, N1—C1 = 1.509(2) Å, N1—C9 = 1.507(3) Å, N1—C4 = 1.515(3) Å, N1—H1 = 0.90(3) Å, N2—H2 = 0.97(3) Å. In the case of $(CAP\text{-}H_3)^{3+}$, the principal bond distances are P2—C11 = 1.836(3) Å, P2—C12 = 1.821(3) Å, P2—C10 = 1.831(3) Å, C12—N6 = 1.491(4) Å, C10—N4 = 1.489(4) Å, N4—H4 = 0.90(4) Å, N5—H5 = 1.01(4) Å, N6—H6 = 0.95(5) Å.

In summary, the principal differences in the reactivities of the two free phosphines can be outlined as follows: i) protonation: with both ligands protonation occurs at the nitrogen atoms, but for PTA only at one single nitrogen, while CAP can be protonated to all three nitrogen atoms; ii) oxidation of P atom: the corresponding P-oxides of both phosphines are easily obtained, but under different reaction conditions, i.e. in the presence of H_2O_2, HNO_3 or N_2O_4 in the case of PTA, in aqueous solution in air with catalytic amounts of Cu^{2+} salt in the case of CAP. The latter, if reacted with H_2O_2 forms the P-oxide dihydroxyammonium dication derivative; iii) methylation: PTA is directly alkylated only at the nitrogen atom, on the contrary CAP is primarily alkylated at phosphorus and subsequently at nitrogen atoms.

4. Synthesis of PTA- and CAP-metal complexes and their use in catalysis

In the last twenty years, the coordination chemistry of PTA has attracted the interest of many research groups worldwide and a great number of complexes with most of the transition metals has appeared in the literature [4]. In order to reduce the environmental impact of industrial chemical processes, the development of metal complexes to be used as catalysts in water or aqueous biphasic processes has gained new interest. In most cases, these water-soluble complexes are obtained by introducing charged or neutral hydrophilic ligands, including PTA [26]. Up to now, much less investigated is the coordination chemistry to transition metals involving CAP due to its very recent synthesis but, considering its structural similarity to PTA as well as its unusual stereoelectronic properties, also this aminophosphine becomes an interesting candidate as ligand for novel water-soluble metal complexes. Many PTA complexes have been applied as excellent catalysts in processes such as hydration of nitriles and alkynes and in redox isomerization of allylic alcohols [4a-c]. As until now no examples are known with CAP analogues, these processes will not be here discussed. The aim of this section

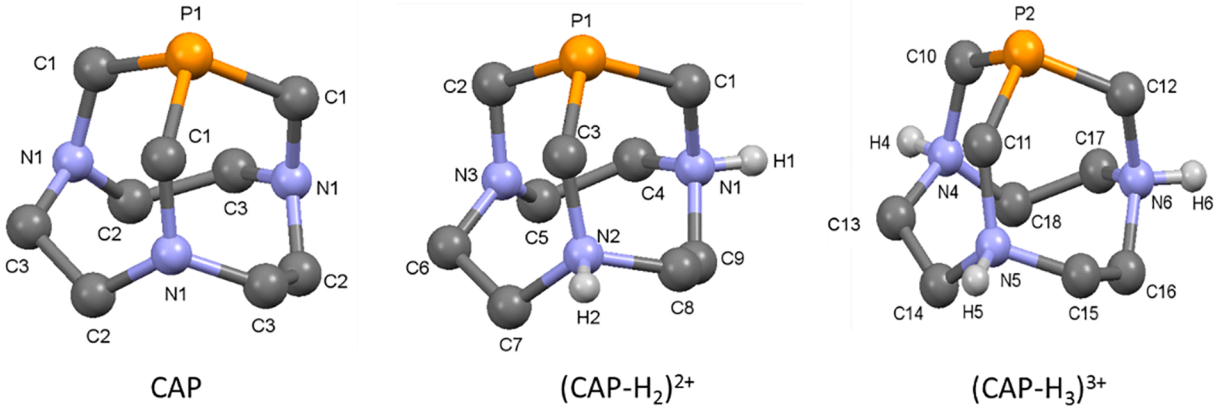

Fig. 5. X-ray crystal structures of cationic units of $CAP\text{-}H_2$ and $CAP\text{-}H_3$, showing the comparison with CAP. Drawings by CCDC Mercury® 3.9.

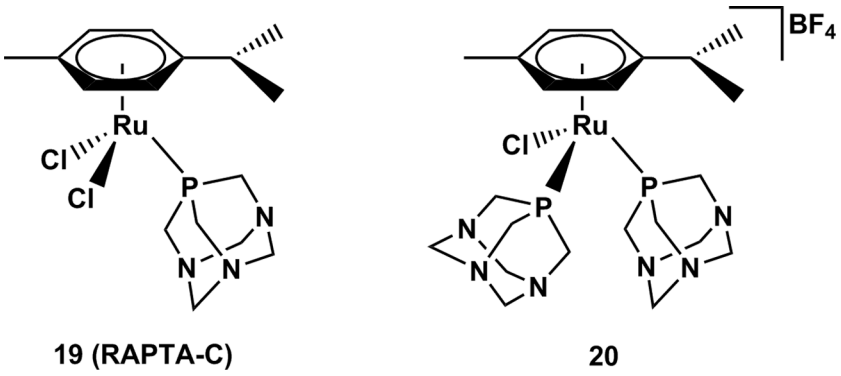

Fig. 6. Drawings of complexes **19** and **20**.

is to describe the synthesis and characterization of coordination compounds of **1** and **2** reported so far in the literature, comparing the results obtained in the same catalytic reactions.

4.1. Ruthenium PTA and CAP complexes as catalysts for transfer hydrogenation

The importance of ruthenium complexes as homogeneous catalysts has been largely demonstrated in the literature [27] and, due to their high reactivity and selectivity, they have been used in various catalytic transformations such as in the hydrogenation of different unsaturated substrates [28]. Among the wide variety of coordination compounds bearing PTA and some of its derivatives, a dominant role is certainly played by ruthenium complexes which have shown interesting catalytic ability and medicinal properties [4]. The advantages of using PTA-based Ru-complexes in catalytic hydrogenation of C═C, C═O and C═N bonds are due to their ability to be used in aqueous phase or biphasic media under mild reaction conditions, such as transfer hydrogenation protocols, with use of the easy-to-handle sodium formate as hydrogen donor [29].

A class of catalytically active PTA compounds is represented by half-sandwich arene complexes, such as $[RuCl_2(\eta^6\text{-}p\text{-cymene})(PTA)]$ (**19**, also known as RAPTA-C) and $[RuCl(\eta^6\text{-}p\text{-cymene})(PTA)_2]BF_4$ (**20**) (Fig. 6) [30]. The former was obtained in high yields by refluxing for 5 h a methanol solution of the dimer $[RuCl_2(\eta^6\text{-}p\text{-cymene})]_2$ in the presence of two equiv. of PTA [31], whereas **20** was prepared by adding one equiv. of PTA to a CH_2Cl_2 solution of **19** followed by the addition of $AgBF_4$ [30]. Both compounds showed to be active in catalytic hydrogenation of numerous substituted arenes into the corresponding cyclohexanes under hydrogen pressure in biphasic conditions [30,32].

The RAPTA-C analogue containing ligand CAP, namely $[RuCl_2(\eta^6\text{-}p\text{-cymene})(CAP)]$ (**21**, RACAP-C), was synthesized in 87% yield by reacting $[RuCl_2(\eta^6\text{-}p\text{-cymene})]_2$ with two equiv. of CAP in CH_2Cl_2 at room temperature (Scheme 4) [10]. The $^{31}P\{^1H\}$ NMR of **21** in $CDCl_3$ shows a singlet at 52.8 ppm, a chemical shift value very different from that of **19** (−36.6 ppm) [31], but in line with the gold(I) CAP derivative $[(CAP\text{-}H_2)_3Au]^{7+}$ characterized by a singlet at 50.9 ppm [6]. The solubility of **21** in water results to be $S(H_2O)_{25°C} = 0.86$ g/L, much lower than that of RAPTA-C [$S(H_2O)_{25°C} = 10$ g/L]. The two cationic derivatives $[RuCl(\eta^6\text{-}p\text{-cymene})(MeCN)(CAP)]PF_6$ (**22**) and $[RuCl(\eta^6\text{-}p\text{-cymene})(CAP)_2]PF_6$ (**23**) were respectively obtained by chloride abstraction from RACAP-C with $TlPF_6$ followed by the addition of MeCN or of a second equivalent of CAP (Scheme 4) [10]. The $^{31}P\{^1H\}$ NMR spectrum of complex **22** exhibits a singlet at 48.2 ppm due to the P atom of CAP and a septet at −144.3 ppm ($J_{PF} = 707.8$ Hz) corresponding to the PF_6^- anion. Similar chemical shift values are observed in the case of the $^{31}P\{^1H\}$ NMR spectrum in acetone-d_6 of **23** with a singlet at 51.6 ppm, corresponding to the two equivalent phosphines, and a septet at −144.3 ppm ($J_{PF} = 707.5$ Hz) for the PF_6^- group. Both ionic complexes show a water solubility slightly higher than **21** with values of 1.1 g/L for **22** and 1.2 g/L for **23** [10].

Single-crystals of **21** and **23** suitable for X-ray diffraction analysis were obtained by diffusion of dry EtOH in a CH_2Cl_2 solution of each complex. The molecular structure of **21** (Fig. 7) consists of a Ru center coordinated by a η^6-p-cymene unit, two Cl atoms, and a κ^1-P coordinated CAP ligand, that keeps the [333] conformation as in the free ligand. The P—N and N—N bond distances of CAP in **21** range from 2.824 to 2.808 Å and from 3.028 to 3.064 Å, respectively. These values are comparable to those observed for free CAP (P-N = 2.886 Å, N-N = 3.1132 Å). The Ru—P bond length in **21** is significantly longer than in the analogous

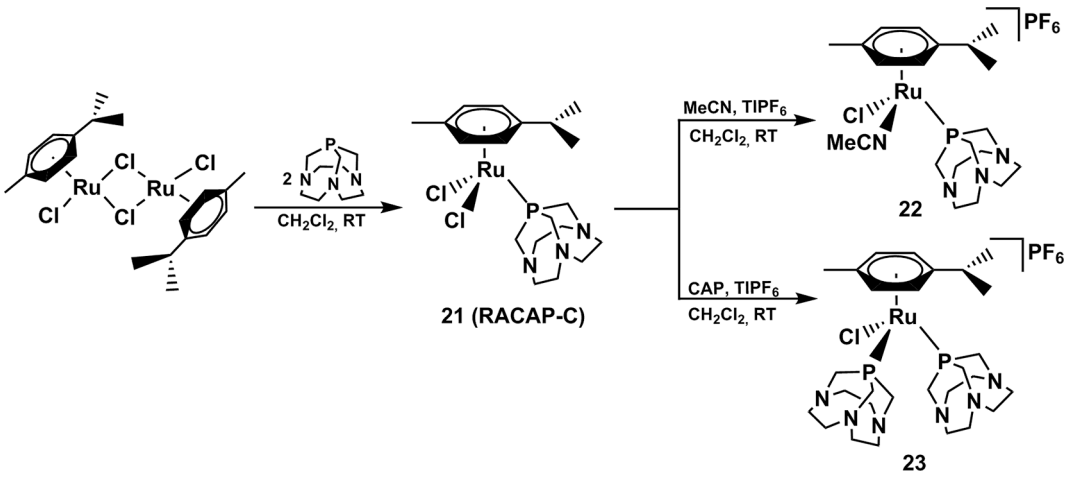

Scheme 4. Synthesis of Ru(II)-arene complexes **22** and **23**.

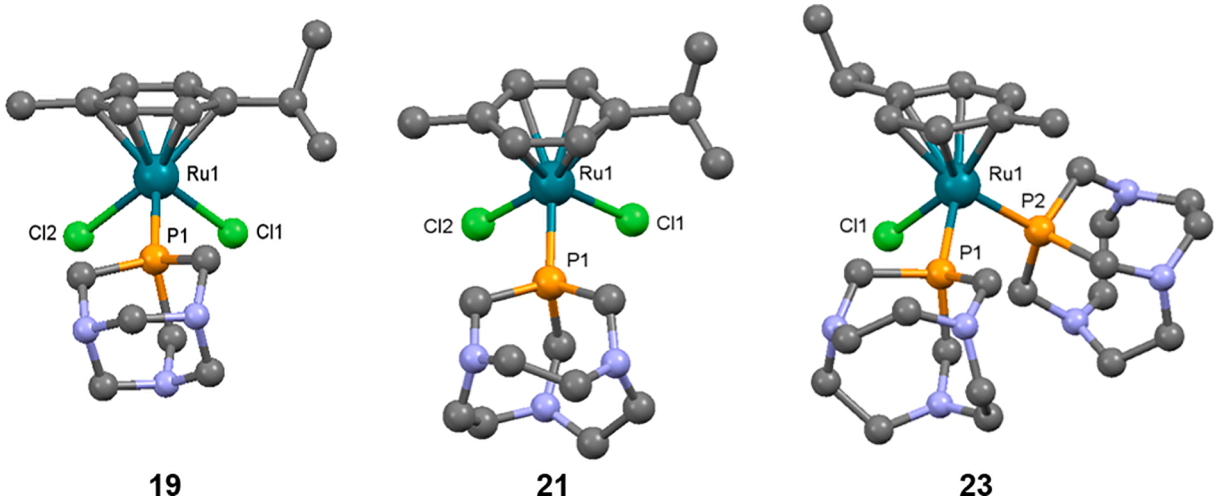

Fig. 7. X-ray crystal structures of complexes **19**, **22** and **23**. Drawings by CCDC Mercury® 3.9.

Table 2
Catalytic transfer hydrogenations with complexes **19** and **21**–**23** [33].

Catalyst	Substrate	Main product	T (°C)	% Conv. (time h)[b]	% Select. to product
19[a]	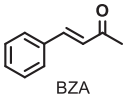 BZA	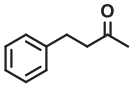 4-phenyl-2-butanone	80	99.5 (24)	93.7
19[c]	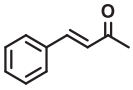	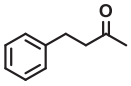	80	30.0 (24)	79.3
21[a]	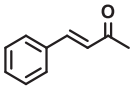	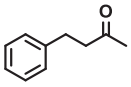	80	99.4 (4)	82.5
21[c]	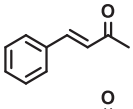	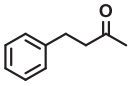	80	76.3 (4)	80.9
22[a]	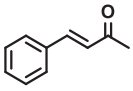	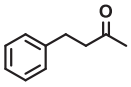	80	82.6 (4)	83.4
22[c]	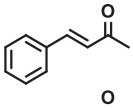	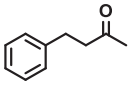	80	51.9 (4)	77.8
23[a]	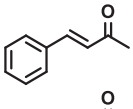	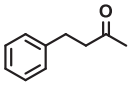	80	71.8 (24) 96.0 (48)	72.8 71.6
23[c]	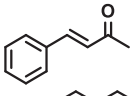	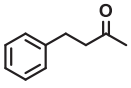	80	66.5 (24) 92.5 (48)	70.1 79.5
23[d]	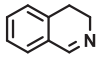 3,4-dihydroisoquinoline	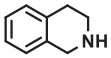 1,2,3,4-tetrahydroisoquinoline	60	10.9 (24)	100
23[d]	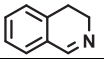	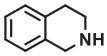	80	74.1 (24) 92.5 (48)	100

[a] Conditions: catalyst, 9×10^{-3} mmol; BZA, 0.98 mmol, HCOONa, 9.8 mmol; MeOH/H_2O (1:1), 6 mL.
[b] Based on GC values of pure samples.
[c] Hg(0) added (poisoning test).
[d] Conditions: catalyst, 1.0×10^{-2} mmol; substrate, 1.0 mmol. HCOONa, 10.0 mmol; MeOH/H_2O, (1:1) 6 mL.

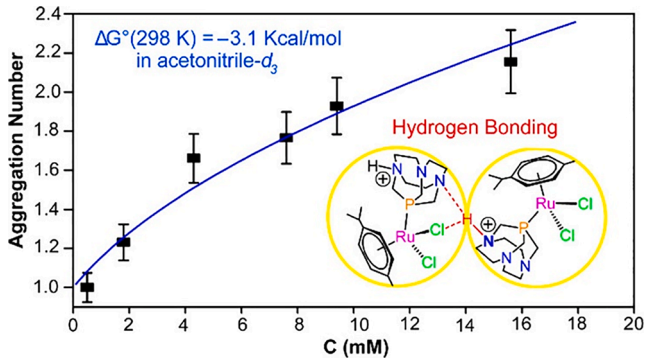

Fig. 8. Graph of aggregation number versus cationic species concentration for **26**. Reprinted with permission from [34]. Copyright 2020 American Chemical Society.

RAPTA [2.3180(5) vs 2.296(2) and 2.298(2) Å], and the same behavior is observed for Ru—C(p-cymene) bond lengths [2.198(2) and 2.275(2) Å in **21** versus 2.179(9) and 2.210(10) Å in RAPTA]. In the case of **23**, the substitution of a Cl–anion with a molecule of CAP ligand causes an elongation of the Ru—P [2.3180(5) Å for **21** vs 2.3254(7) and 2.3353(7) Å for **23**] and Ru—C(p-cymene) centroid [1.709 Å for **21** vs 1.768 Å for **23**] bonds. The Ru—Cl bond shortens from 2.4205(5) Å in **21** to 2.4026 (7) Å in **23** (Fig. 7).

RAPTA-C and complexes **21**–**23** were tested as homogeneous catalysts for the hydrogenation of benzylidene acetone (BZA), selected as model substrate for α,β-unsaturated ketones hydrogenation, using the transfer hydrogenation (TH) protocol involving HCOONa as reducing agent [33]. HCOONa represents one of the mildest reductants for transfer hydrogenation, with a large compatibility with most of the functional groups and is very soluble in water. All the catalytic tests were carried out with a catalyst/BZA/HCOONa ratio of 1/100/1000 at 60° and 80 °C temperatures in water/methanol (1/1) mixture. The addition of the alcohol is mandatory to ensure complete solubility of all reagents, in particular the organic substrate. Selected results are summarized in Table 2.

In the hydrogenation of BZA, the complexes **19**–**22** resulted to be active at 80 °C giving conversions higher than 82% after 24 h and selectivities higher than 80% to the C=C bond hydrogenation, with formation of the saturated ketone (4-phenyl-2-butanone). Hg(0) poisoning tests showed a substantial decrease of conversions with all complexes and in particular with **22**, indicating a certain degree of decomposition of these catalysts under the conditions applied. On the contrary, the catalytic activity of complex **23** was only slightly reduced in the presence of Hg(0) (from 96.0% to 92.5 after 48 h), suggesting a higher stability of this catalyst under the reaction conditions used. This in turn requires a longer reaction time to achieve almost complete conversion after 48 h at 80 °C, with a 71.6% chemoselectivity to 4-phenyl-2-butanone.

On the basis of the observed higher stability, complex **23** was tested also as catalyst for C=N bond hydrogenation of some selected cyclic imines under the same reaction conditions applied for BZA (catalyst/substrate/HCOONa = 1/100/1000, MeOH/H_2O 1:1, 60–80 °C). The best results were observed with 3,4-dihydroisoquinoline as substrate, obtaining a 92.5% conversion to 1,2,3,4-tetrahydroisoquinoline after 48 h at 80 °C (Table 2). Preliminary mechanistic studies carried out by NMR spectroscopy with complex **23** under pseudo-catalytic conditions showed the formation of the monohydride [RuH(η^6-*p*-cymene)(CAP)$_2$]PF_6 (**24**) as the likely catalytically active species [33].

Finally, the self aggregation properties of the Ru-CAP complexes were investigated by means of PGSE (Pulsed field Gradient Spin–Echo) NMR diffusion techniques in acetonitrile solution, together with the monoprotonated species [$RuCl_2$(η^6-*p*-cymene)(PTA-H)](BPh_4) (**25**) and [$RuCl_2$(η^6-*p*-cymene)(CAP-H)](BPh_4) (**26**) [34]. Complex **25** was obtained as an orange solid by reacting **19** at first with an aqueous solution of HCl (0.1 M) and then with a saturated solution of $NaBPh_4$ in methanol [35]. A similar procedure was used in the case of compound **26**, starting from **21**. In details, [$RuCl_2$(η^6-*p*-cymene)(CAP-H)]Cl was at first obtained from the reaction of RACAP-C with a solution of HCl (1 M) and then the counterion exchange from Cl^- to BPh_4^- was accomplished by treating the chloride complex with a small excess of $NaBPh_4$ (1.6 equiv.) in a EtOH/H_2O (16/1) mixture [34]. Whereas complexes **19**, **21**–**23** do not exhibit any tendency to self-aggregate either in acetonitrile-d_3 or in acetone-d_6 solutions, in contrast the monoprotonated compounds **25** and **26** give remarkable self-aggregation in a polar solvent such as acetonitrile-d_3. This process has a rather small self-aggregation free energy calculated by diffusion NMR techniques ($\Delta G^0_{298\ k} = -3.0/-3.1$ kcal mol^{-1}) and involves almost exclusively the cations, leading to the formation of dicationic species through intermolecular hydrogen bonding (HBs). The intercationic hydrogen bonding formation, mostly involving the protonated —NH units, is further supported by the detection of dinuclear species **25**$^+$/**21** in acetonitrile-d_3 solutions containing equimolar mixtures of **25** and **21** [34]. This behavior is

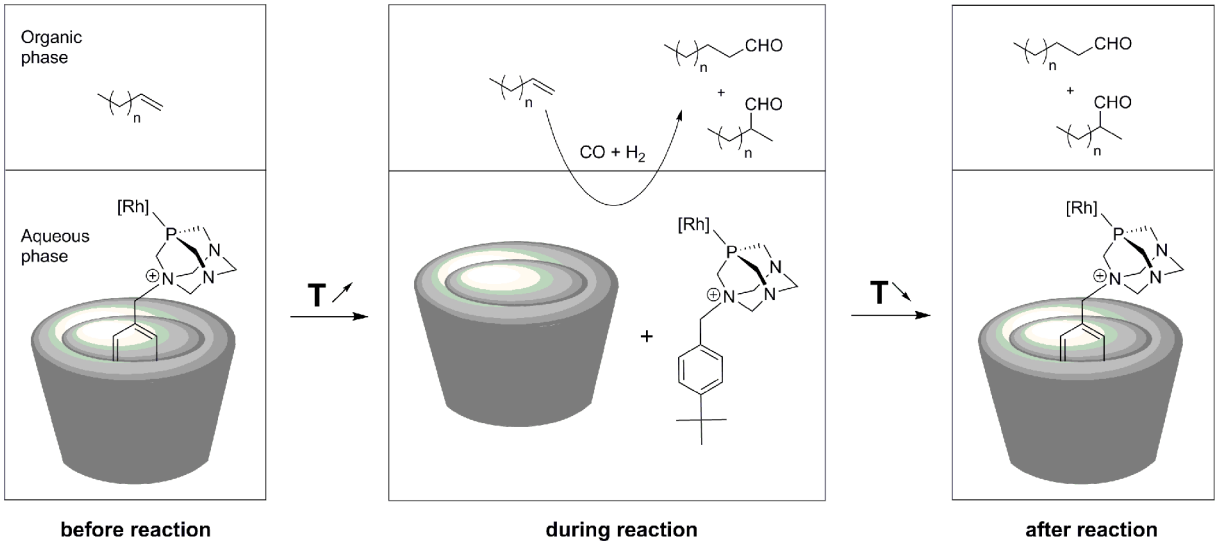

Scheme 5. Thermocontrolled hydroformylation reaction catalyzed by the system [Rh(acac)(CO)$_2$]/[*N*-*tert*-butyl-Bz-PTA]Br. Reprinted with permission from [41]. Copyright 2011 The Royal Society of Chemistry.

particularly interesting as it represents the first case in which a purely dicationic species held together by HBs has been detected in acetonitrile, contrary to what observed for other half-sandwich ruthenium(II) complexes [36], where the anionic units are mostly involved in the formation of ionic aggregates (Fig. 8).

4.2. Rhodium-catalyzed olefin hydroformylation in the presence of PTA and CAP

Transition metal catalyzed alkene hydroformylation represents one of the most important methods to produce aldehydes [37]. A paradigm example of such reaction, carried out in biphasic water-organic solvent system, is represented by the Ruhrchemie/Rhône-Poulenc process, industrially used to obtain butanal from propene in biphasic system under CO/H_2 pressure with a rhodium catalyst stabilized in water by the sodium salt of trisulphonated triphenylphosphine (TPPTS) [38]. The use of water soluble ligands is indeed attractive not only from the environmental point of view, but also due to their ability to immobilize rhodium species in the aqueous phase thus allowing an easy catalyst separation and reuse [39].

Numerous rhodium complexes bearing PTA and its *N*-derivatives have been tested as catalysts for olefin hydroformylation in homogeneous or biphasic conditions 4. As a recent example, PTA and the *N*-benzylated derivative [*N*-Bz-PTA]Cl have been applied in Rh-catalyzed hydroformylation of 1-decene in aqueous phase in the presence of the randomly methylated β-cyclodextrin (RAME-β-CD) [40]. The latter works as mass transfer promoter between the water phase containing the catalyst and the organic phase composed by the olefin. The catalytic runs, performed at temperatures in the range 80–120 °C, showed higher chemoselectivities to aldehydes and higher linear to branched aldehyde (l/b) ratios, compared to the benchmark ligand TPPTS. In fact, at difference with TPPTS, PTA and [*N*-Bz-PTA]Cl can be considered as non-interacting phosphines with RAME-β-CD having association constants equal to zero, thus giving a beneficial effect on the catalytic performances. A thermocontrolled process was observed in aqueous biphasic hydroformylations of 1-decene, 1-dodecene and 1-tetradecene catalyzed by the system $[Rh(acac)(CO)_2]$/ [*N-tert*-butyl-Bz-PTA]Br (acac = acetylacetonate) in the presence of RAME-β-CD [41]. High conversions and chemoselectivities to aldehydes were obtained with all olefin substrates at 100–120 °C temperatures, when the interaction between the phosphine and the cyclodextrin was very low, allowing an increase of the concentration of free catalytic system at the aqueous/organic interface. At the end of the reaction, the decrease of temperature caused the formation of a supramolecular complex between [*N-tert*-butyl-Bz-PTA]Br and RAME-β-CD, leading to a rapid decantation of the biphasic system and thus the easy product separation and catalyst recovery and recycle (Scheme 5).

More recently, CAP has been applied to stabilize Rh(I) species derived from $[Rh(acac)(CO)_2]$ as catalysts for styrene and selected aliphatic olefins hydroformylation, and its activity was compared to that of PTA under the same conditions [42]. In the case of styrene, the system $[Rh(acac)(CO)_2]$/CAP (1:2) gave higher conversion (60%) and higher branched to linear regioselectivity (b/l = 94:6) in toluene/water at 80 °C than the system $[Rh(acac)(CO)_2]$/PTA (1:2) (conversion, 17%; b/l = 55:45). By increasing the CAP:Rh ratio to 3:1, conversions up to 78% were observed, while raising the temperature to 100 °C resulted in worse results both in terms of activity and of regioselectivity. $[Rh(acac)(CO)_2]$/CAP (1:2) gave better results compared to the PTA-based system also in the aqueous hydroformylation of 1-hexene at 80 °C under a CO/H_2 total pressure of 20 bar, with a conversion of 55% versus 13% obtained with PTA. In addition, under these conditions the system favored the formation of linear aldehydes (b/l = 29:71) and demonstrated to be recyclable, remaining active for six consecutive runs without loss in performance. Regardless of the olefin used, the Rh(I)-CAP catalytic system showed to be highly chemoselective, producing aldehydes as the unique products of the reaction from which it could be easily separated by simple decantation of the organic layer.

Table 3
Cytotoxicity (IC_{50}, μM, 72 h)[a] of CAP, **19** and **21**–**23** to selected cell lines [10].

Compound	A2780	A2780cisR	HEK293	Reference
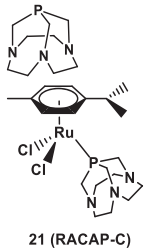	>200	>200	>200	[10]
21 (RACAP-C)	55.3 ± 18.6	108 ± 10	102 ± 26	[10]
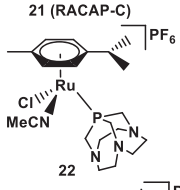 22	65.2 ± 18.0	70.6 ± 3.1	163 ± 46	[10]
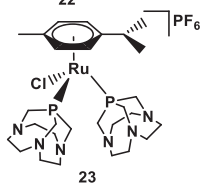 23	48.1 ± 2.2	99.2 ± 15.9	80.7 ± 12.4	[10]
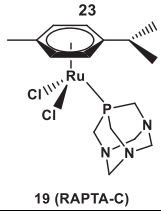 19 (RAPTA-C)	230	270	>1000	[54]

[a] Determined using the MTT (3-(4,5-dimethyl-2-thiazolyl)-2,5-diphenyl-2H-tetrazolium bromide) cell viability assay.

5. Use of PTA and CAP compounds in medicinal chemistry

After the discovery of cisplatin in 1965 as anticancer drug [43], the interest in the development of metallodrugs to be used in diagnostics and in therapy has continually increased [44]. Both their biological activity and their selectivity are greatly dependent on the nature of the metal centre and the choice of coordinating ligands [45]. Many metallodrugs contain phosphine ligands as the strong metal-phosphorus bond makes the complexes highly stable under physiological conditions and, in this context, PTA and CAP, combining P and N donor atoms, are particularly interesting. Whereas the P atom is coordinated to the metal centre, the N atoms remain available for acid-base interactions varying the complexes hydrophilicity depending on pH, thus influencing the biodistribution of the metallodrugs.

Although numerous copper(II) [46] and silver(I) [47] complexes are used, among others, in therapy for antimicrobial and antifungal activity, the design of metallodrugs is mainly focused on their use as anticancer drugs. One of the most common transition metal used for this purpose is ruthenium, thanks to its wide range of oxidation states (Ru^{II}, Ru^{III} and Ru^{IV}) compatible with biological conditions and its lower toxicity compared to platinum [48]. The latter feature is assured by the ability of ruthenium to mimic iron in binding serum proteins such as transferrin and albumin, thus reducing its toxicity and increasing its selectivity to cancer cells where the transferrin receptors are more expressed than in healthy cells [49].

Among the numerous Ru-PTA coordination complexes prepared for this scope, a series of the so-called RAPTA-type arene compounds $[RuCl_2(\eta^6\text{-arene})(PTA)]$ is able to inhibit significantly secondary tumor growth in different cell lines [50]. For this class of compounds, the

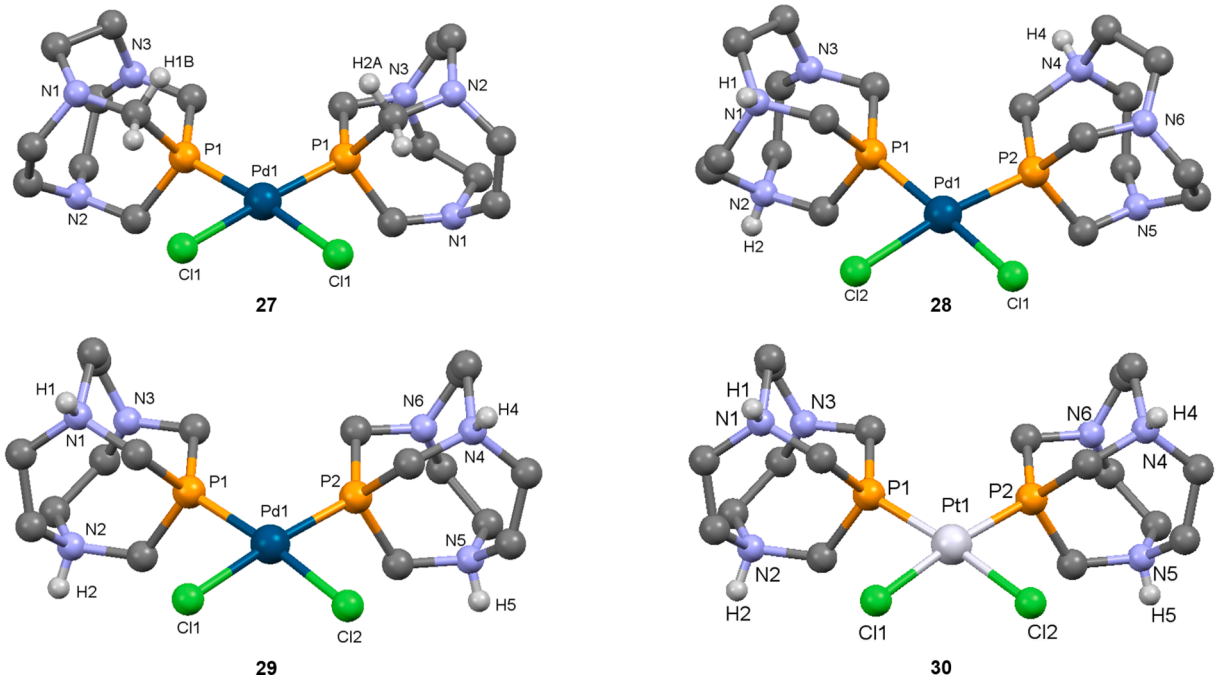

Fig. 9. X-ray crystal structures of complexes **27**–**30**. Anions and solvent molecules omitted for clarity. Drawings by CCDC Mercury® 3.9.

activity and stability, as well as the target recognition and their uptake into cancer cells, strongly depend on the choice of the phosphine ligand. Indeed, PTA derivatives, used instead of pristine PTA, have sometimes led to higher cytotoxicity but at the same time to a lower selectivity [51]. Some of these complexes have also been encapsulated into polymeric matrixes or degradable micelles with the aim to obtain macromolecular complexes with increased drug resistance, solubility and cell uptake [52].

The benchmark compound for RAPTA-type metallodrugs is RAPTA-C (**19**) which showed strong antiangiogenic and antimetastatic activities at moderate doses [53], together with a low general toxicity and a good tolerance to low pH [54]. This property is particularly important, making it more selective against tumor cells which have generally more acidic environment as consequence of a higher metabolic activity, and also suitable for investigation as orally administration drug. Furthermore, complementary pharmacokinetic studies on **19** indicated that ruthenium is rapidly eliminated from the organs and bloodstream.

The cytotoxicity of CAP and its ruthenium complexes **21**–**23** was investigated in vitro and compared to that of RAPTA-C. The stabilities of **21**–**23** under pseudopharmacological conditions have been firstly determined by monitoring every 24 h by ^{1}H and ^{31}P{^{1}H} NMR a 100 mM solution of each compound in NaCl/D_2O at 37 °C [10]. While complex

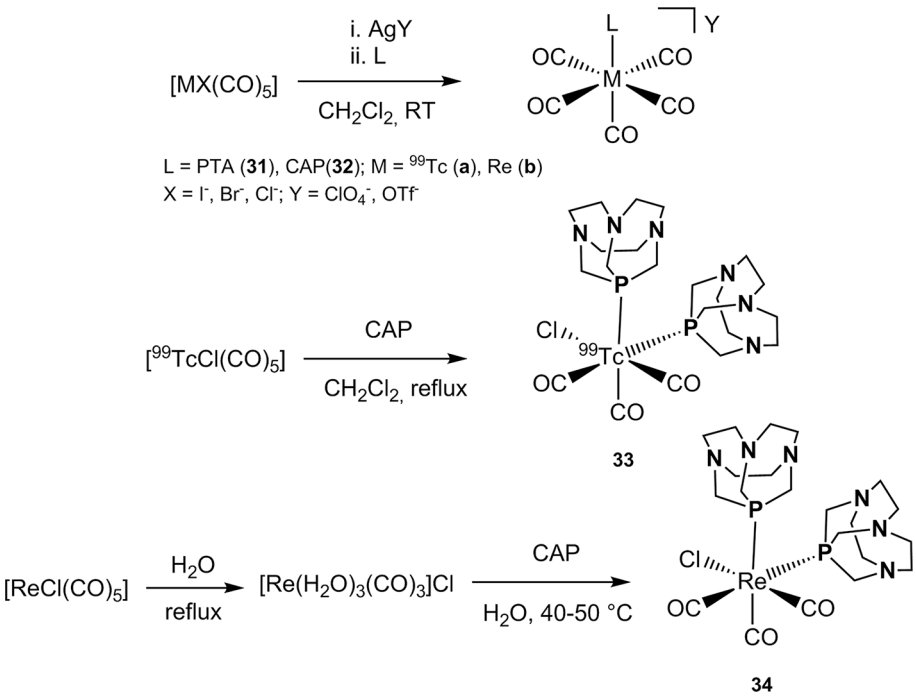

Scheme 6. Synthesis of ^{99}Tc and Re-PTA and CAP complexes **31**–**34**.

21 remains stable under these conditions showing the same NMR signals after 72 h, both ionic derivatives **22** and **23** give partial exchange of MeCN with Cl^- in **22** and of CAP with Cl^- in **23**, with the formation of complex **21** in solution. The cytotoxicity of CAP, **19** and **21**–**23** was evaluated against selected cell lines, in particular against the human ovarian A2780 carcinoma cells, the A2780cisR variant with acquired resistance to cisplatin and against non-cancerous human embryonic kidney cells HEK293 (Table 3). Whereas free CAP showed only minor cytotoxic effects on all the three cell lines tested, all complexes **21**–**23** induced a dose- and cell-dependent decrease in cell viability assays. In particular, **22** showed equal cytotoxicity against both A2780 and A2780cisR cells. The similar IC_{50} values of all ruthenium CAP complexes are likely due to the formation of the same species in solution (**21**) as previously demonstrated by stability tests. Furthermore, all complexes **21**–**23** maintain their cancer cell selectivity by a 2-fold higher growth inhibition effect on A2780 cancer cells compared to noncancerous HEK293 cells and are considerably more active toward all tumor cell lines compared to RAPTA-C.

More recently, it was also demonstrated that substitution of PTA with CAP in square-planar palladium(II) and platinum(II) complexes of formula *cis*-$[MCl_2L_2]$ can lead to the enhancement of their cytotoxicity against HeLa cervical cancer cells [55]. Complexes *cis*-$[PdCl_2(CAP)_2]\cdot 2H_2O$ (**27**), *cis*-$[PdCl_2(CAP\text{-}H)(CAP\text{-}H_2)]Cl_3\cdot 3H_2O$ (**28**), *cis*-$[PdCl_2(CAP\text{-}H_2)_2]Cl_4\cdot 4.5H_2O$ (**29**) and *cis*-$[PtCl_2(CAP\text{-}H_2)_2]Cl_4\cdot 4.5H_2O$ (**30**) were synthesized and characterized both in solution and in the solid state (Fig. 9). The latter analysis, together with DFT calculations refinements and quantum theory of atoms-in-molecules (QTAIM) based analysis revealed the occurrence of interligand $C—H^{\sigma+}\cdots{}^{\sigma+}H—C$ interactions (hydrogen-hydrogen bonds) between the phosphine cages. These interactions produce a stabilizing effect and are sufficiently strong to overcome ligand-ligand repulsions due to the bulky aminophosphine cages. In **27** and **30**, the pseudo-eclipsed alignment of the CAP cages in the *cis* geometry results in significant ligand-ligand repulsion, with an expansion of P-M-P angle from the expected 90° to 101° in **27**.

As for platinum(II) PTA complexes [56], complex **30** possesses low cytotoxicity and selectivity, whereas the palladium(II) derivative **27** showed a cytotoxic activity comparable to that of cisplatin against HeLa cells, albeit it resulted to be poorly selective [55].

Finally, the pentacarbonyl complexes of formula $[M(PTA)(CO)_5]X$ (**31**) and $[M(CAP)(CO)_5]X$ [**32**, M = ^{99}Tc (a), Re (b); X = ClO_4^-, OTf^-] together with the tricarbonyl CAP compounds $[^{99}TcCl(CAP)_2(CO)_3]$ (**33**) and $[ReCl(CAP)_2(CO)_3]$ (**34**) have been very recently reported [57]. The aim of this study was to prepare water-soluble ^{99}Tc(I) and Re(I) compounds and to evaluate their stability under pseudo-biological conditions for their potential use in nuclear medicine. It is well known that technetium-99 m is the most used radionuclide as diagnostic tool and rhenium-188/186 radionuclides show good results in radiotherapy. All pentacarbonyl complexes have been prepared by the reaction of $[MX(CO)_5]$ (M= ^{99}Tc or Re; X = ClO_4^- or OTf^-) with PTA and CAP in dichloromethane at room temperature, while **33** and **34** were synthesized starting from the metal precursors $[TcCl(CO)_5]$ and $[Re(H_2O)_3(CO)_3]Cl$, either in refluxing CH_2Cl_2 or in water at 40–50 °C, respectively (Scheme 6).

The PTA complexes are soluble in water at neutral pH, whereas the CAP derivatives are not soluble at pH = 7 but readily dissolve after acidification with dilute acids (pH = 3). Furthermore, both PTA and CAP complexes showed a good stability for at least 24 h in a simulated biological medium where an excess of histidine was added as competitive coordinating ligand ("histidine challenge reaction"). All compounds showed to be resistant under these conditions and no ligand-to-histidine exchange was found, making them particularly interesting as potential radiopharmaceutical drugs [58].

CRediT authorship contribution statement

Antonella Guerriero: Conceptualization, Data curation, Writing - original draft. **Luca Gonsalvi:** Supervision, Writing - review & editing, Funding acquisition.

Declaration of Competing Interest

The authors declare that they have no known competing financial interests or personal relationships that could have appeared to influence the work reported in this paper.

Acknowledgement

CNR financial contribution through project ORCAS (project code DCM.AD004.063.001) is gratefully acknowledged.

References

[1] P.T. Anastas, W. Leitner, P.G. Jessop, J.-C. Li, P. Wasserscheid, A. Stark, Handbook of green chemistry: green solvents, Eds. Wiley-VCH: Weinheim, Germany, 2010.
[2] F. Kerton, R. Mariott, Alternative solvents for green chemistry, 2nd Edition RSC Green Chem. Ser. 20 (2013) 1–350, https://doi.org/10.1039/9781849736824.
[3] K.H. Shaughnessy, Hydrophilic ligands and their application in aqueous-phase metal-catalyzed reactions, Chem. Rev. 109 (2009) 643–710, https://doi.org/10.1021/cr800403r.
[4] (a) A.D. Phillips, L. Gonsalvi, A. Romerosa, F. Vizza, M. Peruzzini, Coordination Chemistry of 1,3,5-triaza-7-phosphatricyclo[3.3.1.1]decane (PTA) Transition metal complexes and related catalytic, medicinal and photoluminescent applications, Coord. Chem. Rev. 248 (2004) 955–993, doi: 10.1016/j.ccr.2004.03.010. (b) J. Bravo, S. Bolano, L. Gonsalvi, M. Peruzzini, Coordination chemistry of 1,3,5-triaza-7-phosphaadamantane (PTA) and derivatives. Part II. The quest for tailored ligands, complexes and related applications, Coord. Chem. Rev. 254 (2010) 555–607, doi: 10.1016/j.ccr.2009.08.006. (c) A. Guerriero, M. Peruzzini, L. Gonsalvi, Coordination Chemistry of 1,3,5-triaza-7-phosphatricyclo [3.3.1.1]decane (PTA) and derivatives. Part III. Variations on a theme: Novel architectures, materials and applications, Coord. Chem. Rev. 355 (2018) 328–361, doi: 10.1016/j.ccr.2017.09.024. (d) A.G. Mahmoud, M.F.C. Guedes da Silva, A.J.L. Pombeiro. 3,7-Diacetyl-1,3,7-triaza-5-phosphabicyclo[3.3.1]nonane (DAPTA) and derivatives: Coordination chemistry and applications. Coord. Chem. Rev. (2020), in press. doi: 10.1016/j.ccr.2020.213614.
[5] L. Gonsalvi, A. Guerriero, F. Hapiot, D.A. Krogstad, E. Monflier, G. Reginato, M. Peruzzini, Lower- and upper-rim-modified derivatives of 1,3,5-triaza-7-phosphaadamantane: Coordination chemistry and applications in catalytic reactions in water, Pure Appl. Chem. 85 (2013) 385–396, 1351/PAC-CON-12-07-10.
[6] S.N. Britvin, A. Lotnyk, Water-soluble phosphine capable of dissolving elemental gold: the missed link between 1,3,5-triaza-7- phosphaadamantane (PTA) and Verkade's ephemeral Ligand, J. Am. Chem. Soc. 137 (2015) 5526–5535, https://doi.org/10.1021/jacs.5b01851.
[7] D.J. Daigle, A.B. Pepperman, S.L. Vail, Synthesis of a monophosphorus analog of hexamethylenetetramine, J. Heterocycl. Chem. 11 (1974) 407–408, https://doi.org/10.1002/jhet.5570110326.
[8] D.J. Daigle, T.J. Decuir, J.B. Robertson, D.J. Darensbourg, 1,3,5-triaza-7-phosphatricyclo[3.3.1.1(3,7)]decane and derivatives, Inorg. Synth. 32 (1998) 40–45, https://doi.org/10.1002/9780470132630.ch6.
[9] D.W. White, B.A. Karcher, R.A. Jacobson, J.G. Verkade, Tris(dialkylamino) phosphine with pyramidal nitro gens, J. Am. Chem. Soc. 101 (1979) 4921–4925, https://doi.org/10.1021/ja00511a022.
[10] A. Guerriero, W. Oberhauser, T. Riedel, M. Peruzzini, P.J. Dyson, L. Gonsalvi, New class of half-sandwich ruthenium(II) arene complexes bearing the water-soluble CAP ligand as an in vitro anticancer agent, Inorg. Chem. 56 (2017) 5514–5518, https://doi.org/10.1021/acs.inorgchem.7b00915.
[11] S.N. Britvin, A.M. Rumyantsev, A.E. Zobnina, M.V. Padkina, Between adamantane and atrane: intrabridgehead interactions in the cage-like phosphane related to a novel tris(homoadamantane) ring system, Chem. Eur. J. 22 (2016) 14227–14235, https://doi.org/10.1002/chem.201601637.
[12] a) J. Dale, Exploratory calculations of medium and large rings. 1. Conformational minima of cycloalkanes, Acta Chem. Scand. 27 (1973) 1115–1129, https://doi.org/10.3891/acta.chem.scand.27-1115;
b) J. Dale, Exploratory calculations of medium and large rings.2. Conformational interconversions in cycloalkanes, Acta Chem. Scand. 27 (1973) 1130–1148, https://doi.org/10.3891/acta.chem.scand.27-1130.
[13] a) H. Koyama, T. Yoshino, Syntheses of some medium sized cyclic triamines and their cobalt(III) complexes, Bull. Chem.: Soc. Jpn. 45 (1972) 481, https://doi.org/10.1246/bcsj.45.481;
b) P.J.A. Ribeiro-Claro, A.M. Amado, M.P.M. Marques, J.J.C. Teixeira-Dias, Ab initio SCF MO calculations on triaza and tetraaza cyclic amines, J. Chem. Soc. Perkin Trans. 2 (1996) 1161–1167, https://doi.org/10.1039/p29960001161.
[14] a) D.J. Darensbourg, J.B. Robertson, D.L. Larkins, J.H. Reibenspies, Water-soluble organometallic compounds. 7. Further studies of 1,3,5-triaza-7-phosphaadamantane derivatives of group 10 metals, including metal carbonyls and hydrides, Inorg. Chem. 38 (1999) 2473–2481, https://doi.org/10.1021/ic981243j;
b) K.J. Fisher, E.C. Alyea, N. Shahnazarian, A P-31 NMR-study of the water-

soluble derivatives of 1,3,5-triaza-7-phosphaadamantane (PTA), Phosphorus Sulfur Silicon Related Elements 48 (1990) 37–40, https://doi.org/10.1080/10426509008045879.

[15] a) J.C.A. Boeyens, S.M. Dobson, R.D. Hancock, Structures of bis(1-thia-4,7-diazacyclononane)copper(II) nitrate and bis(1,7-diaza-4-thiaheptane)copper(II) nitrate - A different conformation for the coordinated macrocycle, Inorg. Chem. 24 (1985) 3073–3076, https://doi.org/10.1021/ic00213a041;
b) D.G. Evans, J.C.A. Boeyens, The conformation of 9-membered rings, Acta Crystallog. B 46 (1990) 524–532, https://doi.org/10.1107/S0108768190000878.

[16] R.J. Puddephatt, The Chemistry of Gold, Topics in inorganic and general chemistry, Elsevier, Amsterdam, 1978, doi: 10.1080/00945717808057442.

[17] a) V.I. Siele, Some reactions of 1,3,5-triaza-7-phosphaadamantane and its 7-oxide, J. Heterocycl. Chem. 14 (1977) 337–339, https://doi.org/10.1002/jhet.5570140238;
b) D.J. Daigle, A.B. Pepperman, Chemical proof for preferred nitrogen quarternization in 1,3,5-triaza-7-phosphaadamantane, J. Heterocycl. Chem. 12 (1975) 579–580, https://doi.org/10.1002/jhet.5570120328.

[18] E. Nicolas, A. Guerriero, V. Lyaskovsky, M. Peruzzini, K. Lammertsma, L. Gonsalvi, J.C. Slootweg, Metal-free reduction of phosphine oxides using polymethylhydrosiloxane, Inorganics 4 (2016) 34–41, https://doi.org/10.3390/inorganics4040034.

[19] D. Bernier, U.K. Wefelscheid, S. Woodward, Properties, preparation and synthetic uses of amine N-oxides. An update, Org. Prep. Proced. Int.: New J. Org. Synth. 41 (2009) 173–210, https://doi.org/10.1080/00304940902955756.

[20] A. Mena-Cruz, P. Lorenzo-Luis, A. Romerosa, M. Saoud, M. Serrano-Ruiz, Synthesis of the water soluble ligands dmPTA and dmoPTA and the complex [RuClCp(HdmoPTA)(PPh_3)](OSO_2CF_3) (dmPTA=N, N''-dimethyl-1,3,5-triaza-7-phosphaadamantane, dmoPTA=3,7-dimethyl-1,3,7-triaza-5-phosphabicyclo[3.3.1]nonane, HdmoPTA=3,7-H-3,7-dimethyl-1,3,7-triaza-5-phosphabicyclo[3.3.1]nonane), Inorg. Chem. 46 (2007) 6120–6128, https://doi.org/10.1021/ic070168m.

[21] J.M. Forward, R.J. Staples, C.W. Liu, J.P. Fackler, Luminescent tris(3-ethyl-1,5-diaza-3-azonia-7-phosphatricyclo[3.3.1.13,7]decane-*P*)gold(I) tetraiodide trihydrate, [$(EtTPA)_3Au]I_4.3H_2O$, Acta Cryst. C 53 (1997) 195–197, https://doi.org/10.1107/S0108270196012486.

[22] E. Fluck, J.E. Förster, J. Weidlein, E. Hädicke, 1,3,5-triaza-7-phosphaadamantane (monophospha-urotropine), Z. Naturforsch. 32 (1977) 499–506.

[23] J.M. Forward, R.J. Staples, J.P. Fackler, Crystal structure of 1-n-butyliodo-1-azonia-3,5-diaza-7-phosphaadamantane iodide, ($C_6H_{12}PN_3(CH_2)_4$)I)I, Z. Kristallogr. 211 (1996) 129–130.

[24] a) B. Assmann, K. Angermaier, H. Schmidbaur, Synthesis, structure and complexes of a new bicyclic N, P-ligand derived from phosphatriazaadamantane, J. Chem. Soc. Chem. Commun. (1994) 941–942, https://doi.org/10.1039/c39940000941;
b) B. Assmann, K. Angermaier, M. Paul, J. Riede, H. Schmidbaur, Synthesis of 7-alkyl/aryl-1,3,5-triaza-7-phosphonia-adamantane cations and their reductive cleavage to novel N-methyl-P-alkyl/aryl[3.3.1]bicyclononane ligands, Chem. Ber. 128 (1995) 891–900, https://doi.org/10.1002/cber.19951280907.

[25] K.H. Jogun, J.J. Stezowski, E. Fluck, H.J. Weissgraeber, Molecular-structure of 7-methyl-1,3,5-triaza-7-phosphaadamantane-7-ium-tetrafluoroborate - Preparation and characterization of 7-methyl-1,3,5-triaza-7-phospha-tricyclo[3,3,2,13,7]-undecan-7-ium-iodide, Z. Naturforsch. B 33 (1978) 1257–1262.

[26] (a) U.M. Lindstroem, Organic reactions in water: principles, strategies and applications, Eds. Wiley-Blackwell Publishing, Oxford, UK, 2007. (b) B.R. James, F. Lorenzini, Developments in the chemistry of tris(hydroxymethyl)phosphine, Coord. Chem. Rev. 254 (2010) 420–430, doi: 10.1016/j.ccr.2009.07.008.

[27] (a) R.H. Morris, Ruthenium and Osmium, in: J.G. de Vries, Elsevier (Eds.), The handbook of homogeneous hydrogenation, Wiley-VHC Verlag GmbH & Co. KGaA, Weinheim Germany, 2007, 45-70, ISBN: 978-3-527-31161-3. (b) S.E. Clapham, A. Hadzovic, R.H. Morris, Mechanism of the H2-hydrogenation and transfer hydrogenation of polar bonds catalyzed by ruthenium hydride complexes, Coord. Chem. Rev. 248 (2004), 2201–2237, doi: 10.1016/j.ccr.2004.04.007. (c) D. Evans, J.A. Osborn, F.H. Jardine, G. Wilkinson, Homogeneous hydrogenation and hydroformylation using ruthenium complexes, Nature 208 (1965) 1203–1204, doi: 10.1038/2081203b0.

[28] a) A. Zanotti-Gerosa, W. Hems, M. Groarke, F. Hancock, Ruthenium-catalysed asymmetric reduction of setone, Platin. Met. Rev. 49 (2005) 158–165, https://doi.org/10.1595/147106705X75421;
b) M.L. Clarke, M.B. Diaz-Valenzuela, A.M.Z. Slawin, Hydrogenation of aldehydes, esters, imines, and ketones catalyzed by ruthenium complexes of a chiral tridentate ligand, Organometallics 26 (2007) 16–19, https://doi.org/10.1021/om060673b.

[29] (a) D.J. Darensbourg, F. Joo, M. Kannisto, A. Katho, J.H. Reibenspies, D.J. Daigle, Water-soluble organometallic compounds. 4. Catalytic-hydrogenation of aldehydes in an aqueous 2-phase solvent system using a 1,3,5-triaza-7-phosphaadamantane complex of ruthenium, Inorg. Chem, 33 (1994) 200–208, doi: 10.1021/ic00080a006. (b) D.J. Darensbourg, F. Joo, M. Kannisto, A. Katho, J.H. Reibenspies, Water-soluble organometallic compounds. 2. Catalytic-hydrogenation of aldehydes and olefins by new water-soluble 1,3,5-triaza-7-phosphaadamantane complexes of ruthenium and rhodium, Organometallics 11 (1992) 1990–1993, doi: 10.1021/om00042a006.

[30] P.J. Dyson, D.J. Ellis, G. Laurenczy, Minor modifications to the ligands surrounding a ruthenium complex lead to major differences in the way in which they catalyse the hydrogenation of arenes, Adv. Synth. Catal. 345 (2003) 211–215, https://doi.org/10.1002/adsc.200390014.

[31] C.S. Allardyce, P.J. Dyson, D.J. Ellis, S.L. Heath, [Ru(η^6-*p*-cymene)Cl_2(pta)] (pta=1,3,5-triaza-7-phosphatricyclo[3.3.1.1]decane): a water soluble compound that exhibits pH dependent DNA binding providing selectivity for diseased cells, Chem. Commun. 2 (2001) 1396–1397, https://doi.org/10.1039/b104021a.

[32] P.J. Dyson, D.J. Ellis, W. Henderson, G. Laurenczy, A comparison of ruthenium-catalysed arene hydrogenation reactions in water and 1-alkyl-3-methylimidazolium tetrafluoroborate ionic liquids, Adv. Synth. Catal. 345 (2003) 216–221, https://doi.org/10.1002/adsc.200390015.

[33] A. Guerriero, M. Peruzzini, L. Gonsalvi, Ruthenium(II)-arene complexes of the water-soluble ligand CAP as catalysts for homogeneous transfer hydrogenations in aqueous phase, Catalysts 8 (2018) 88, https://doi.org/10.3390/catal8020088.

[34] L. Sian, A. Guerriero, M. Peruzzini, C. Zuccaccia, L. Gonsalvi, A. Macchioni, Diffusion NMR Studies on the self-aggregation of Ru-arene CAP complexes: evidence for the formation of H-bonded dicationic species in acetonitrile, Organometallics 39 (2020) 941–948, https://doi.org/10.1021/acs.organomet.9b00703.

[35] S. Bolaño, G. Ciancaleoni, J. Bravo, L. Gonsalvi, A. Macchioni, M. Peruzzini, PGSE NMR studies on RAPTA derivatives: evidence for the formation of H-bonded dicationic species, Organometallics 27 (2008) 1649–1652, https://doi.org/10.1021/om701131s.

[36] a) D. Zuccaccia, A. Macchioni, An accurate methodology to identify the level of aggregation in solution by PSGE NMR measurements: the case of half-sandwich diamino ruthenium(II) salts, Organometallics 24 (2005) 3476–3486, https://doi.org/10.1021/om050145k;
b) D. Zuccaccia, G. Bellachioma, G. Cardaci, G. Ciancaleoni, C. Zuccaccia, E. Clot, A. Macchioni, Interionic structure of ions pair and ion quadruples of half-sandwich ruthenium(II) salts bearing α-diimine ligands, Organometallics 26 (2007) 3930–3946, https://doi.org/10.1021/om7003157.

[37] a) M. Beller, B. Cornils, C.D. Frohning, C.W. Kohlpaintner, Progress in hydroformylation and carbonylation, J. Mol. Catal. A: Chem. 104 (1995) 17–85, https://doi.org/10.1016/1381-1169(95)00130-1;
b) H.-W. Bohner, B. Cornils, Hydroformylation of alkenes: an industrial view of the status and importance, Adv. Catal. 47 (2002) 1–64, https://doi.org/10.1016/S0360-0564(02)47005-8.

[38] B. Cornils, E.G. Kuntz, Introducing TPPTS and related ligands for industrial biphasic processes, J. Organomet. Chem. 502 (1995) 177–186, https://doi.org/10.1016/0022-328X(95)05820-F.

[39] A.M. Trzeciak, J.J. Ziolkowski, Perspectives of rhodium organometallic catalysis. Fundamental and applied aspects of hydroformylation, Coord. Chem. Rev. 190 (1999) 883–900, https://doi.org/10.1016/S0010-8545(99)00127-7.

[40] F.-X. Legrand, F. Hapiot, S. Tilloy, A. Guerriero, M. Peruzzini, L. Gonsalvi, E. Monflier, Aqueous rhodium-catalyzed hydroformylation of 1-decene in the presence of randomnly methylated β-cyclodextrin and 1,3,5-triaza-7-phosphaadamantane derivatives, Appl. Catal. A: General 362 (2009) 62–66, https://doi.org/10.1016/j.apcata.2009.04.0147.

[41] N. Six, A. Guerriero, D. Landy, M. Peruzzini, L. Gonsalvi, F. Hapiot, E. Monflier, Supramolecularly controlled surface activity o fan amphiphilic ligand. Application onto aqueous biphasic hydroformylation of higher olefins, Catal. Sci. Technol. 1 (2011) 1347–1353, https://doi.org/10.1039/c1cy00156f.

[42] O.L. Eliseev, T.N. Bondarenko, S.N. Britvin, P.P. Khodorchenko, A.L. Lapidus, Efficient water-soluble catalytic system Rh^{I}-CAP for biphasic hydroformylation of olefins, Mendeleev Commun. 28 (2018) 264–266, https://doi.org/10.1016/j.mencom.2018.05.011.

[43] a) B. Rosenberg, L. Van Camp, T. Krigas, Inhibition of cell division in Escherichia Coli by electrolysis products from a platinum electrode, Nature 205 (1965) 698–699, https://doi.org/10.1038/205698a0;
b) B. Rosenberg, L. Van Camp, J.E. Trosko, V.H. Mansour, Platinum compounds: a new class of potent antitumor agents, Nature 222 (1969) 385–386, https://doi.org/10.1038/222385a0.

[44] P. Martins, M. Marques, L. Coito, A.J.L. Pombeiro, P.V. Baptista, A.R. Fernandes, Organometallic compounds in cancer therapy: past lessons and future directions, Anti-Cancer Agents Med. Chem. 14 (2014) 1199–1212, https://doi.org/10.2174/1871520614666140829124925.

[45] A.R. Kapdi, I.J.S. Fairlamb, Anti-cancer palladium complexes: a focus on PdX_2L_2, palladacycles and related complexes, Chem. Soc. Rev. 43 (2014) 4751–4777, https://doi.org/10.1039/c4cs00063c.

[46] A. Drzewiecka-Antonik, P. Rejmak, M.T. Klepka, A. Wolska, P. Pietrzyk, K. Stepien, G. Sanna, M. Struga, Synthesis, structural studies and biological activity of novel Cu(II) complexes with thiourea derivatives of 4-azatricyclo[5.2.1.02,6]dec-8-ene-3,5-dione, J. Inorg. Biochem. 176 (2017) 8–16, https://doi.org/10.1016/j.jinorgbio.2017.08.001.

[47] V.T. Yilmaz, C. Icsel, J. Batur, S. Aydinlik, P. Sahinturk, M. Aygun, Structures and biochemical evaluation of silver(I) 5,5-diethylbarbiturate complexes with bis(diphenylphosphino)alkanes as potential antimicrobial and anticancer agents, Eur. J. Med. Chem. 139 (2017) 901–916, https://doi.org/10.1016/j.ejmech.2017.08.062.

[48] a) M.J. Clarke, Ruthenium metallopharmaceuticals, Coord. Chem. Rev. 236 (2003) 209–233, https://doi.org/10.1016/S0010-8545(02)00312-0;
b) W.H. Ang, A. Casini, G. Sava, P.J. Dyson, Organometallic ruthenium-based antitumor compounds with novel modes of action, J. Organomet. Chem. 696 (2011) 989–998, https://doi.org/10.1016/j.jorganchem.2010.11.009.

[49] A.R. Timerbaev, C.G. Hartinger, S.S. Aleksenko, B.K. Keppler, Interactions of antitumor metallodrugs with serum proteins: advances in characterization using modern analytical methodology, Chem. Rev. 106 (2006) 2224–2248, https://doi.org/10.1021/cr040704h.

[50] a) A.A. Nazarov, C.G. Hartinger, P.J. Dyson, Opening the lid on piano-stool complexes: an account of ruthenium(II)-arene complexes with medicinal applications, J. Organomet. Chem. 751 (2014) 251–260, https://doi.org/10.1016/

j.jorganchem.2013.09.016;
b) B.S. Murray, M.V. Babak, C.G. Hartinger, P.J. Dyson, The development of RAPTA compounds for the treatment of tumors, Coord. Chem. Rev. 306 (2016) 86–114, https://doi.org/10.1016/j.ccr.2015.06.014.

[51] A.L. Noffke, A. Habtemariam, A.M. Pizarro, P.J. Sadler, Designing organometallic compounds for catalysis and therapy, Chem. Commun. 48 (2012) 5219–5246, https://doi.org/10.1039/C2CC30678F.

[52] a) B.M. Blunden, D.S. Thomas, M.H. Stenzel, Macromolecular ruthenium complexes as anti-cancer agents, Polym. Chem. 3 (2012) 2964–2975, https://doi.org/10.1039/C2PY20439H;
b) H. Lu, B.M. Blunden, W. Scarano, M. Lu, M.H. Stenzel, Anti-metastatic effects of RAPTA-C conjugated polymeric micelles on two-dimensional (2D) breast tumor cells and three-dimensional (3D) multicellular tumor spheroids, Acta Biomater. 32 (2016) 68–76, https://doi.org/10.1016/j.actbio.2015.12.020.

[53] a) A. Weiss, R.H. Berndsen, M. Dubois, C. Müller, R. Schibli, A.W. Griffioen, P. J. Dyson, P. Nowak-Sliwinska, In vivo antitumor activity of the organometallic ruthenium(II)-arene complex [Ru(η^6-p-cymeneCl2(PTA)] (RAPTA-C) in human ovarian and colorectal carcinomas, Chem. Sci. 5 (2014) 4742–4748, https://doi.org/10.1039/C4SC01255K;
b) P. Nowak-Sliwinska, J.R. van Beijnum, A. Casini, A.A. Nazarov, G. Wagnières, H. van den Bergh, P.J. Dyson, A.W. Griffioen, Organometallic ruthenium(II) arene compounds with antiangiogenic activity, J. Med. Chem. 54 (2011) 3895–3902, https://doi.org/10.1021/jm2002074.

[54] C. Gossens, A. Dorcier, P.J. Dyson, U. Rothlisberger, pKa estimation of ruthenium (II)-arene PTA complexes and their hydrolysis products via a DFT/continuum electrostatics approach, Organometallics 26 (2007) 3969–3975, https://doi.org/10.1021/om700364s.

[55] S.N. Britvin, A.M. Rumyantsev, A.A. Silyutina, M.V. Padkina, Palladium(II) and platinum(II) complexes of novel water-soluble phosphane CAP: structure, interligand hydrogen-hydrogen bonding and in vitro cytotoxicity, ChemistrySelect 2 (2017) 8721–8725, https://doi.org/10.1002/slct.201701819.

[56] P. Bergamini, V. Bertolasi, L. Marvelli, A. Canella, R. Gavioli, N. Mantovani, S. Manas, A. Romerosa, Phosphinic platinum complexes with 8-thiotheophylline derivatives: synthesis, characterization, and antiproliferative activity, Inorg. Chem. 46 (2007) 4267–4276, https://doi.org/10.1021/ic062133c.

[57] A.E. Miroslavov, S.N. Britvin, H. Brandad, R. Alberto, E.S. Stepanova, A. P. Shevyakova, G.V. Sidorenko, Water-soluble carbonyl complexes of ^{99}Tc(I) and Re(I) with adamantane-cage aminophosphines PTA and CAP, J. Organomet. Chem. 896 (2019) 83–89, https://doi.org/10.1016/j.jorganchem.2019.05.029.

[58] K.J. Kiplin, C.M. Clavel, F. Edafe, P.J. Dyson, Naphthalimide-tagged ruthenium-arene anticancer complexes: combining coordination with intercalation, Organometallics 31 (2012) 7031–7039, https://doi.org/10.1021/om3007079.